Asian Journal of Current Research in Clinical Cancer
ISSN: 3062-4444
2024, Volume 4, Issue 1, Page No: 90-100

Available online at: www.galaxypub.co/page/journals

Galaxy Publication

Preclinical Evaluation of the PSMA/GRPR-Targeting Heterodimer [68Ga]Ga-BQ7812 for PET Imaging of Prostate Cancer: Advancing Toward Clinical Translation

E. Tursunov[1*], G. Karimova[1], D. Akbarov[1]

[1]Department of Clinical Oncology, Faculty of Medicine, Tashkent State Medical Academy, Tashkent, Uzbekistan.

***E-mail** ✉ tashkent.clinonc.53@outlook.com

Received: 06 January 2024; **Revised:** 29 March 2024; **Accepted:** 04 April 2024

ABSTRACT

Radioligands that target prostate-specific membrane antigen (PSMA) and gastrin-releasing peptide receptor (GRPR) have emerged as promising tools for both imaging and therapeutic strategies in prostate cancer. Yet, heterogeneous expression of these receptors in tumors and metastatic lesions can limit the effectiveness of single-target approaches. To address this limitation, dual-targeting radioligands capable of simultaneously binding PSMA and GRPR have been developed. In this study, we report the preclinical evaluation of [68Ga]Ga-BQ7812, a PSMA/GRPR heterodimer designed for PET-based diagnostic imaging of prostate cancer, with the goal of supporting its clinical translation. In vitro assays using PSMA/GRPR-positive PC3-pip cells demonstrated rapid and selective binding to both targets. Biodistribution studies in PC3-pip xenograft-bearing mice revealed highest uptake at 1 hour post-injection in tumor tissue (PSMA+/GRPR+, 10.4 ± 1.0% IA/g), kidneys (PSMA+, 45 ± 16% IA/g), and pancreas (GRPR+, 5.6 ± 0.7% IA/g). By 3 hours post-injection, tumor-to-background ratios improved, reflecting preferential retention of the radioligand in tumor tissue. Additionally, [68Ga]Ga-BQ7812 exhibited low toxicity and an acceptable estimated dosimetry (effective dose = 0.0083 mSv/MBq), supporting its potential for first-in-human studies and further clinical development.

Keywords: Prostate cancer, GRPR, PSMA, Heterodimer, Molecular imaging, PET imaging

How to Cite This Article: Tursunov E, Karimova G, Akbarov D. Preclinical Evaluation of the PSMA/GRPR-Targeting Heterodimer [68Ga]Ga-BQ7812 for PET Imaging of Prostate Cancer: Advancing Toward Clinical Translation. Asian J Curr Res Clin Cancer. 2024;4(1):90-100. https://doi.org/10.51847/HuPwltXO8d

Introduction

Over the past decade, radiopharmaceutical research has increasingly focused on developing radioligands directed at prostate cancer (PCa)-specific biomarkers, significantly advancing PCa diagnosis and treatment. Two molecular targets that have garnered considerable attention are prostate-specific membrane antigen (PSMA, also known as glutamate carboxypeptidase II) and gastrin-releasing peptide receptor (GRPR). Both receptors are expressed at substantially higher levels in malignant PCa cells than in normal prostate tissue or other healthy organs, making them attractive candidates for diagnostic and therapeutic radiopharmaceutical development [1, 2].

PSMA expression in malignant PCa is markedly elevated, showing 100–1000 times higher levels than those observed in proximal renal tubules, small intestine, salivary glands, and benign prostate tissue. Overexpression persists across all disease stages but generally increases with tumor progression [3, 4]. The most commonly investigated PSMA-targeting ligands are small urea-based pseudo-peptide inhibitors, which have been optimized over the years to enhance binding efficiency and specificity [5-7]. These developments have led to multiple clinical investigations of PSMA-targeted radioligands, yielding promising results. Examples include PET imaging agents [68Ga]Ga-PSMA-11 and [18F]F-DCFPyL, as well as the theranostic pair [68Ga]Ga-PSMA-617/[177Lu]Lu-PSMA-617, all of which have received FDA approval for clinical use [8-12].

GRPR, a G-protein coupled receptor belonging to the bombesin receptor family, is primarily expressed in the pancreas, with only low levels present in the gastrointestinal tract and benign prostate tissue [13]. GRPR activation

induces smooth muscle contraction in the GI tract and has been linked to increased proliferation of cancer cells and tumor growth [14, 15]. Notably, GRPR is overexpressed in a majority of PCa cases (62–100%) and is also present in other malignancies including breast, lung, head and neck, pancreatic, and brain cancers [16, 17]. Unlike PSMA, GRPR expression may decline as PCa progresses due to androgen dependence [3, 13, 18]. Multiple GRPR-targeting radioligands, including both agonists and antagonists, have been developed; while first-generation agonists showed initial promise, second-generation antagonists demonstrated improved tumor uptake, better pharmacokinetics, and reduced off-target effects [19, 20]. Clinical translation of GRPR imaging has been explored with PET ([68Ga]Ga-RM2) and SPECT ([111In]In-RM2) tracers, successfully imaging both primary and metastatic lesions [21, 22].

Although radioligands targeting either PSMA or GRPR have advanced PCa theranostics, their efficacy depends on uniform expression of the target. Tumors and metastases often display heterogeneous expression, with areas lacking PSMA or GRPR, as confirmed by comparative studies using [68Ga]Ga-RM2 and [68Ga]Ga-PSMA-11 in patients with biochemical recurrence [23, 24]. Such heterogeneity has motivated the design of heterodimeric radiotracers capable of simultaneously binding both PSMA and GRPR to potentially improve detection sensitivity. Since the first PSMA/GRPR heterodimers were reported in 2014 [25, 26], multiple derivatives have been developed to enhance imaging sensitivity and specificity over their monomeric counterparts [27–34]. To date, [68Ga]Ga-DOTA-PSMA(Inhibitor)-Lys3-Bombesin remains the only heterodimer evaluated in humans, demonstrating favorable safety and dosimetry, though further clinical validation is required [35]. In 2020, our group reported preclinical data on an [111In]In-BQ7812 heterodimer for SPECT imaging of PCa in murine models, highlighting its promising characteristics [32]. PET imaging offers several advantages over SPECT, including higher sensitivity and resolution, enabling detection of sub-centimeter lesions and improved quantitative capability for therapy planning. Gallium-68 is particularly suitable for PET imaging of peptide-based agents due to its convenient generator-based production, low cost, and 68-minute half-life that matches peptide kinetics [36-38]. Building on this foundation, the present study evaluates the preclinical performance of [68Ga]Ga-BQ7812 to advance the clinical translation of PSMA/GRPR-targeting PET radioligands for prostate cancer.

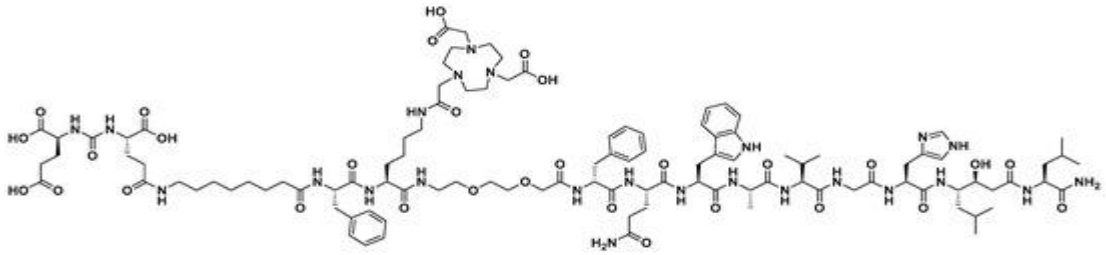

Figure 1. Chemical structure of the PSMA/GRPR-targeting heterodimeric radiotracer BQ7812.

Materials and Methods

Peptide assembly

BQ7812 was produced via solid-phase peptide synthesis (SPPS) on Rink amide resin (0.69 mmol/g loading), following procedures described previously [32]. Coupling reactions employed Oxyma Pure and DIC as activators with DIPEA as a base in DMF, each reaction proceeding for a minimum of three hours. After synthesis, the crude peptide underwent purification using preparative reverse-phase HPLC. The identity and purity of BQ7812 were confirmed via analytical HPLC-MS, with theoretical $[M+2H]^{2+}$ and $[M+3H]^{3+}$ values of 1132.1 and 755.1 and observed values of 1132.0 and 754.9. The purified peptide was lyophilized, reconstituted in Chelex-treated Milli-Q water, and stored at −20 °C.

Radiolabelling with gallium-68

Gallium-68 was eluted from a $^{68}Ge/^{68}Ga$ generator (Cyclotron Co., Obninsk, Russia) using 0.1 M metal-free HCl. For labelling, 2 nmol of BQ7812 in 200 µL sodium acetate buffer (1.25 M, pH 3.6) was mixed with 20 MBq ^{68}Ga and heated at 85 °C for 10 minutes. Radiochemical yields were analyzed by ITLC using 0.2 M citric acid as the mobile phase, and the resulting [68Ga]Ga-BQ7812 was used without further purification.

Stability testing included incubation in human serum at 37 °C, in PBS at room temperature, and in the presence of a 1000-fold molar excess of EDTA. After 1 hour, the integrity of the radioligand was assessed via ITLC. For

scaled radiolabelling suitable for clinical translation, 2 nmol of BQ7812 was combined with 1.5 GBq ^{68}Ga in 0.65 mL sodium acetate buffer (2 M, pH 4.5) and heated at 90 °C for 12 minutes. ITLC was used to check radiochemical purity and colloid formation (NaOAc/MeOH 1:1 and 0.2 M sodium citrate as eluents, respectively). For toxicological studies, 2 nmol BQ7812 was labelled with 100 MBq of ^{68}Ga under identical conditions.

In vitro characterization

All in vitro assays employed the human PC3-pip prostate carcinoma cell line, which co-expresses PSMA and GRPR (provided by Prof. Martin Pomper, Johns Hopkins University, Baltimore, MD, USA). Cells were seeded 24–48 hours prior to experiments at 5–7 × 10^5 per vial, and all experiments were conducted in triplicate.

Assessment of specific binding

To determine the binding specificity of [68Ga]Ga-BQ7812, approximately 3 × 10^6 cells per well were plated in 12-well plates. Blocking studies involved pre-incubating cells for 15 minutes at room temperature with either 750 nM PSMA-11, 750 nM NOTA-PEG2-RM26, or both, followed by addition of 20 nM [68Ga]Ga-BQ7812. After 1 hour at 37 °C, cell-associated radioactivity was quantified using a gamma counter.

Internalization and cellular uptake

For internalization assays, 3 × 10^6 PC3-pip cells per 3 cm Petri dish were incubated with 1 nM [68Ga]Ga-BQ7812 at 37 °C. Cells were collected at 1 and 3 hours to determine total uptake. At 3 hours, the membrane-bound and internalized fractions were separated using the previously described acid/base extraction method [32].

In vivo studies

Ex vivo and imaging experiments were performed using BALB/c nu/nu mice implanted with PC3-pip xenografts. Animal care and experimental procedures followed the Declaration of Helsinki guidelines and were approved by the Ethics Committee for Animal Research in Uppsala, Sweden (5.8.18-00473/2021; approved 26 February 2021).

Biodistribution

To investigate how [68Ga]Ga-BQ7812 distributes across tissues over time, BALB/c nu/nu mice were intravenously injected with 40 pmol of the tracer (1 h pi: 300 kBq/mouse; 3 h pi: 700 kBq/mouse) in a total volume of 100 µL 1% BSA/PBS. Each time point included four animals. At the designated time, mice were anesthetized with a Ketalar–Rompun mixture (20 µL per g body weight; Ketalar 10 mg/mL, Rompun 1 mg/mL) and sacrificed via cardiac puncture. To assess receptor specificity, some animals received co-injection with 5 nmol of either non-labelled NOTA-PEG2-RM26 or PSMA-11 to block GRPR or PSMA, respectively. Following euthanasia, organs were collected, and the radioactivity in each was measured. The average mouse weight in these experiments was 17.4 ± 0.96 g.

PET/CT imaging

PET scans were performed on PC3-pip xenograft-bearing mice using a nanoScan PET/MR1 3T scanner (Mediso, Budapest, Hungary). Animals were injected with 100 pmol [68Ga]Ga-BQ7812 (8 MBq in 100 µL 1% BSA). Immediately after PET acquisition, a CT scan was conducted on a nanoScan SPECT/CT system using the same imaging bed. In the receptor-blocked group, mice were co-administered 5 nmol of both non-labelled NOTA-PEG2-RM26 and PSMA-11 together with the radioligand. PET/CT imaging was performed at 1 and 3 h post-injection for both non-blocked (n = 2) and blocked (n = 2) groups. Images were reconstructed using Nucline nanoScan software version 3.04.014.0000.

Dosimetry

For radiation dosimetry assessment, NMRI mice were injected with 40 pmol [68Ga]Ga-BQ7812 (150–720 kBq in 100 µL 1% BSA). Mice were euthanized at 0.5, 1, 2, and 4 h post-injection, and organ-specific radioactivity was quantified. The mean body weight was 27.4 ± 1.6 g. Absorbed dose calculations were performed using OLINDA/EXM 1.0 software with the adult male phantom model. Mouse organ uptake was extrapolated to human organs using the "percent kg/g" scaling method (Eq. 1), and residence times were determined by integrating the fitted exponential time-activity curves.

$$(\%\mathrm{IA/organ})_{\mathrm{human}} = [(\%\mathrm{IA/g})_{\mathrm{animal}} \times (\mathrm{kBqTBweight})_{\mathrm{animal}} \times (g_{\mathrm{organ}}/(\mathrm{kBqTBweight})_{\mathrm{human}}] \quad (1)$$

Toxicological evaluation

The safety of BQ7812 (Pepmic, China) and its radiolabelled form [68Ga]Ga-BQ7812 was assessed for both acute (within 24 hours) and subacute (up to 28 days) effects in Wistar rats at NAMRC, Russia (Protocol PZ_22_6_Kirichenko AS_V1; ethical approval granted 7 June 2022). Animals were maintained under standard barrier-type housing conditions [39]. Each experimental group consisted of 15 rats (mean weight 427 g), which received a single intravenous dose of either 10.3 µg BQ7812 in 0.2 mL saline, 10.3 µg [68Ga]Ga-BQ7812 (10 MBq) in 0.2 mL saline, 0.2 mL saline alone, or 0.2 mL sodium acetate buffer. The dosage selection for rats was extrapolated from the intended human clinical dose (300 µg for a 75 kg patient, equivalent to 4 mg/kg) using body surface area scaling, resulting in 10.3 µg per rat [(4 µg × 427 g)/1000 g × 6] [40]. Ten animals per group were sacrificed 24 hours post-injection to evaluate acute toxicity, while the remaining five rats were observed for 28 days to assess subacute effects. Body weights were monitored at baseline, at 24 hours post-administration for acute toxicity, and every two days in the subacute study. Blood was collected for biochemical analysis, including alanine aminotransferase, albumin, aspartate aminotransferase, bilirubin, glucose, creatinine, urea, total protein, cholesterol, and ALT. Upon necropsy, organ weights were recorded for the brain, heart, lungs, liver, adrenal glands, kidneys, spleen, testes, and thymus.

Statistical analysis

Data are presented as mean ± standard deviation. Statistical significance was determined using either unpaired two-tailed t-tests or one-way ANOVA followed by Bonferroni correction for multiple comparisons in GraphPad Prism (version 6, GraphPad Software, Windows). A p-value less than 0.05 was considered statistically significant.

Results and Discussion

Synthesis and radiolabelling

BQ7812 **(Figure 1)** was successfully synthesized and efficiently labelled with gallium-68, achieving radiochemical yields between 97–99%. Minimal release of free gallium-68 was observed after incubation in PBS or in the presence of a 1000-fold excess of EDTA for 1 hour, as assessed by ITLC. The compound remained stable in human serum at 37 °C over 1 hour, showing no detectable dissociation of the radiolabel.

In vitro characterization

Binding assays using the PC3-pip cell line confirmed that [68Ga]Ga-BQ7812 binds specifically to both PSMA and GRPR **(Figure 2).** Blocking either PSMA or GRPR individually with PSMA-11 or NOTA-PEG2-RM26 significantly reduced cellular uptake ($p < 0.05$). Pre-treatment with both blockers simultaneously caused an even greater decrease in uptake compared to single-receptor blockade, indicating that both receptors contribute meaningfully to the heterodimer's cellular localization.

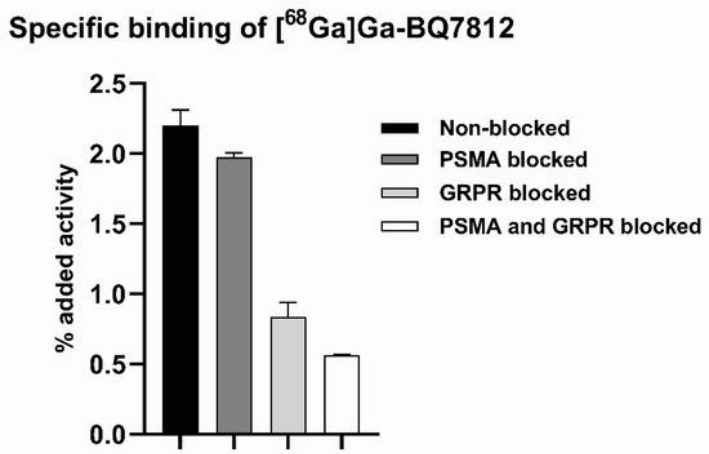

Figure 2. In vitro specificity of [68Ga]Ga-BQ7812 binding. Target blockade was achieved by pre-incubation with non-labelled PSMA-11 and/or NOTA-PEG2-RM26 (500 nM per well). Statistical significance was evaluated using one-way ANOVA with Bonferroni correction for multiple comparisons, revealing significant differences across all experimental conditions.

Analysis of cellular processing of [68Ga]Ga-BQ7812 demonstrated rapid engagement with PSMA and GRPR **(Figure 3)**. At 3 hours post-incubation, approximately 20% of the total cell-associated radioactivity was internalized, while the remaining 80% remained bound to the cell membrane. These findings are consistent with the previously reported cellular processing patterns of [111In]In-BQ7812 [32].

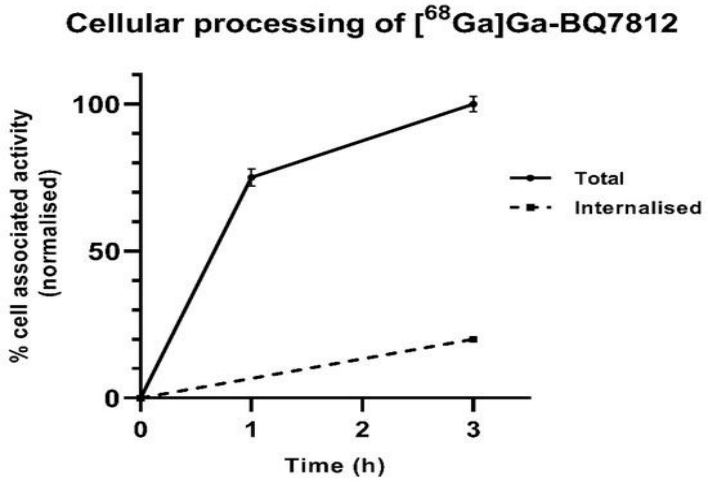

Figure 3. Cellular processing of [^{68}Ga]Ga-BQ7812. Values are normalized to the highest uptake in the experiment.

In vivo characterisation

The in vivo target specificity of [68Ga]Ga-BQ7812 was evaluated in mice bearing PC3-pip xenografts. In the PSMA-blocked group, the uptake of [68Ga]Ga-BQ7812 in both tumors and kidneys was significantly reduced compared to the non-blocked controls. Similarly, GRPR blockade led to a significant decrease in tracer accumulation in the tumors and pancreas relative to non-blocked animals. These findings confirm that [68Ga]Ga-BQ7812 binds specifically to both PSMA and GRPR, as demonstrated by the markedly lower radioactivity in tumors and in normal organs expressing PSMA (kidneys) or GRPR (pancreas) when the respective targets were blocked **(Figure 4)**.

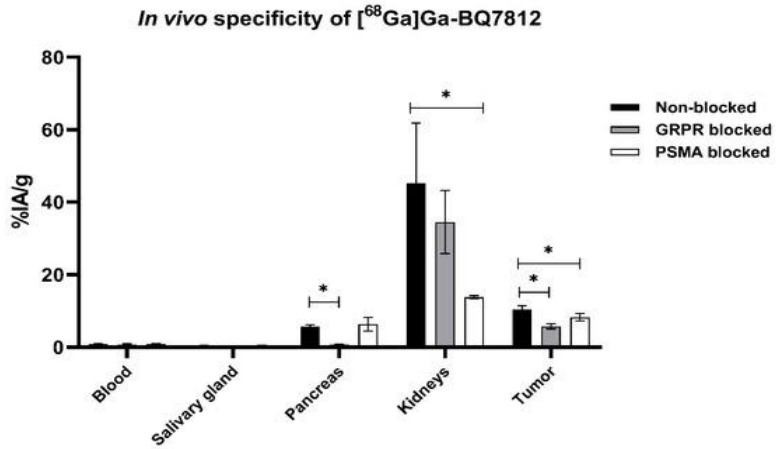

Figure 4. In vivo binding specificity of [^{68}Ga]Ga-BQ7812 towards PSMA and GRPR at 1 h pi in PC3-pip tumour-bearing mice. Co-injection of non-labelled NOTA-PEG$_2$-RM26 (5 nmol/animal) or non-labelled PSMA-11 (5 nmol/animal) to block GRPR and PSMA respectively. Statistical analysis was done using one-way ANOVA with Bonferroni's test corrected for multiple comparisons. * Statistically significant ($p < 0.05$) difference in organ uptake.

The distribution of [68Ga]Ga-BQ7812 in vivo was examined at 1 and 3 hours post-injection in BALB/c nu/nu mice implanted with PC3-pip xenografts. At the 1-hour time point, the compound predominantly accumulated in the tumor (10.4 ± 1.0% IA/g), kidneys (45 ± 16% IA/g), and pancreas (5.6 ± 0.6% IA/g), whereas uptake in other

tissues was minimal, generally ≤1% IA/g **(Figure 5)**. By 3 hours post-injection, overall activity levels declined across most organs, but notable retention remained in the tumor (5.7 ± 0.6% IA/g) and kidneys (12 ± 6% IA/g). Clearance from kidneys and pancreas was proportionally greater than from the tumor, with tumor activity at 3 hours representing roughly 55% of its 1-hour value, while kidneys and pancreas retained only ~26% and ~11% of the earlier uptake, respectively. Analysis of tumor-to-organ (T/O) ratios revealed increased contrast over time for all organs except the liver, with the most pronounced ratios observed for muscle (116 ± 22) and bone (47 ± 13) **(Figure 6)**.

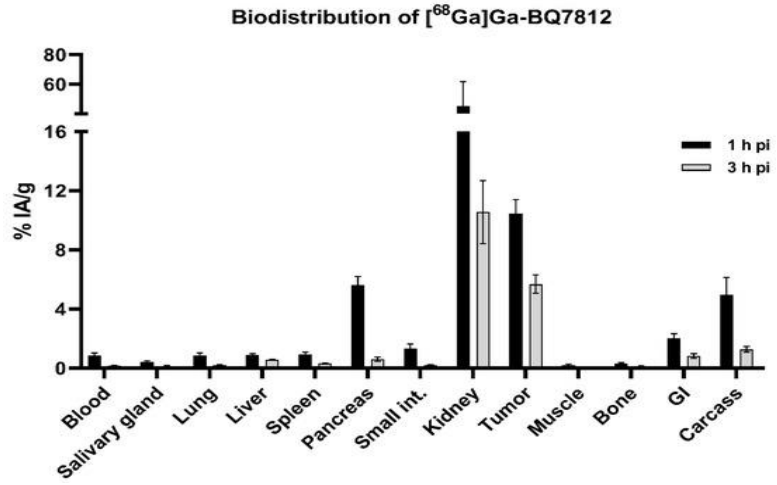

Figure 5. In vivo biodistribution of [^{68}Ga]Ga-BQ7812 in PC3-pip tumour-bearing mice at 1 and 3 h post-injection showing the uptake activity in specified organs.

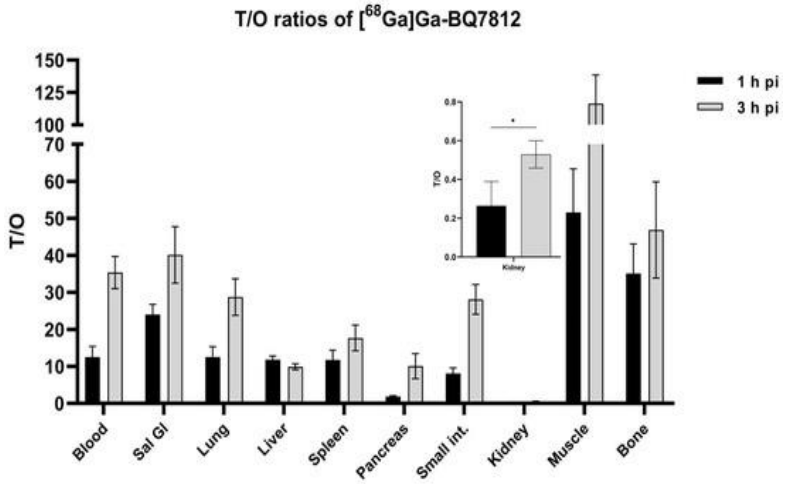

Figure 6. illustrates the in vivo biodistribution of [68Ga]Ga-BQ7812 in PC3-pip tumor-bearing mice at 1 and 3 hours post-injection, highlighting the tumor-to-organ (T/O) ratios. Statistical comparisons were performed using an unpaired, two-tailed t-test, with a significant difference observed for the tumor-to-kidney ratio (*p < 0.05).

Consistent with the ex vivo biodistribution results, nanoScan PET/CT imaging **(Figure 7)** demonstrated prominent radiotracer accumulation in both the tumor and kidneys at 1 and 3 hours post-injection. In the PSMA/GRPR-blocked group, tumor visualization was markedly reduced, and kidney contrast was diminished, confirming target-specific uptake of [68Ga]Ga-BQ7812 in vivo.

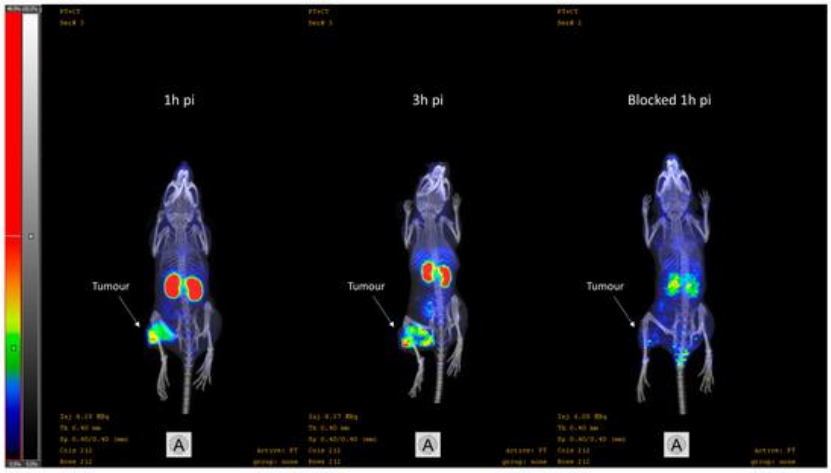

Figure 7. presents representative nanoScan PET/CT images of PC3-pip xenograft-bearing mice following injection of [68Ga]Ga-BQ7812 (100 pmol, 8 MBq). Images show 1 h post-injection on the left, 3 h post-injection in the center, and PSMA/GRPR-blocked mice at 1 h post-injection on the right.

Dosimetry estimates for male patients were derived from the ex vivo mouse biodistribution data using Eq. 1, with organ-specific absorbed doses reported in **Table 1**. The highest estimated doses were observed in the kidneys (0.0660 mGy/MBq), heart wall (0.0265 mGy/MBq), and lower large intestine wall (0.0250 mGy/MBq). Absorbed doses for all other organs and tissues were below 0.02 mSv/MBq, resulting in a total effective dose of 0.0083 mSv/MBq.

Table 1. The absorbed dose (mGy/MBq) of [^{68}Ga]Ga-BQ7812 in each of the targeted organs.

Target Organ	Absorbed Dose (mGy/MBq)
Adrenals	0.0043
Brain	0.0007
Breasts	0.0030
Gallbladder wall	0.0042
Lower large intestine wall	0.0250
Small intestine wall	0.0199
Stomach wall	0.0048
Upper large intestines LI wall	0.0111
Heart wall	0.0265
Kidneys	0.0660
Liver	0.0044
Lungs	0.0041
Muscle	0.0024
Ovaries	0.0045
Pancreas	0.0186
Red marrow	0.0057
Osteogenic cells	0.0080
Skin	0.0026
Spleen	0.0033
Testes	0.0030
Thymus	0.0038
Thyroid	0.0030
Urinary bladder wall	0.0036
Uterus	0.0042
Total body	0.0044
Effective dose equivalent (mSv/MBq)	0.0124
Effective dose (mSv/MBq)	0.0083

The preclinical toxicology evaluation indicated no alterations in clinical or biochemical parameters between the experimental and control groups. Pathomorphological analyses of the adrenal glands, liver, brain, lungs, thymus, spleen, heart, testes, kidneys, and bladder revealed only mild morphological changes in both groups for BQ7812 and [68Ga]Ga-BQ7812. The lack of significant differences in these changes between the experimental and control groups supports the absence of observable toxicity for both the radiolabelled and non-labelled heterodimer.

Discussion

Prostate cancer (PCa) remains the most commonly diagnosed malignancy and a leading cause of cancer-related mortality in men, highlighting the ongoing need for novel diagnostic and therapeutic strategies [40-42]. Radionuclide-based molecular imaging with PET, combined with CT or MRI, offers high sensitivity and spatial resolution, enabling the detection of small lesions. Targeting PCa-specific biomarkers using radioligands has shown substantial potential for accurate diagnosis, staging, and monitoring of treatment responses. Among these biomarkers, PSMA and GRPR are the most extensively studied, with radioligands targeting either receptor demonstrating promising diagnostic and therapeutic outcomes [9-12, 21, 22].

However, heterogeneous expression of PSMA and GRPR, both inter- and intra-patient, can lead to false-negative results and inaccurate staging, thereby potentially limiting treatment efficacy [23, 24, 43]. Bispecific radioligands capable of simultaneously targeting both PSMA and GRPR have been proposed to overcome these limitations. Such heterodimeric radiotracers may enhance specific tumor binding, improve lesion detection in cases of variable receptor expression, and potentially increase therapeutic efficacy through more uniform tracer delivery. Although preclinical studies have reported encouraging results, clinical translation of PSMA/GRPR heterodimers remains limited.

In this study, we present the preclinical evaluation of the PSMA/GRPR-targeting heterodimer [68Ga]Ga-BQ7812 for PET/CT imaging of PCa. In vitro and in vivo experiments demonstrated receptor-specific binding, as evidenced by significant reductions in uptake following pre-saturation of PSMA and/or GRPR (**Figures 2, 4, and 7).** Biodistribution studies revealed preferential uptake in the tumor, along with elevated retention in the kidneys and pancreas at 1 h post-injection, consistent with endogenous expression of PSMA and GRPR in these organs. Over time, tracer uptake decreased across all organs, with the highest residual activity observed in the kidneys (11.7 ± 5.8% IA/g) followed by the tumor (5.7 ± 0.62% IA/g) at 3 h post-injection. Importantly, the reduction of activity in tumors was less pronounced compared to that in normal tissues, resulting in increased tumor-to-kidney and tumor-to-pancreas ratios between 1 and 3 h post-injection **(Figure 6)**. These findings suggest enhanced tumor retention, potentially due to the combined targeting of both receptors.

Despite the favorable tumor retention, the biodistribution profile of [68Ga]Ga-BQ7812 may not be optimal for radiotherapeutic applications, such as labeling with lutetium-177, due to relatively low tumor-to-kidney ratios, which remained below 0.5 at all measured time points for both gallium-68 and indium-111 labeling [32]. Interestingly, our first-generation heterodimer, BQ7800, which had tenfold lower PSMA affinity, showed equivalent tumor and kidney uptake in vivo [31, 32]. This observation may inform future molecular design strategies for heterodimers intended for targeted therapy. Overall, [68Ga]Ga-BQ7812 displayed a biodistribution profile comparable to [111In]In-BQ7812, with the exception of lower liver uptake and retention when labeled with gallium-68.

Although the PSMA/GRPR-heterodimer BQ7812 has previously been evaluated preclinically with indium-111, it is essential to reassess the ligand when using a different radionuclide, as variations in labelling conditions between gallium-68 and indium-111 could impact the reproducibility and quality of the radioligand. Our labelling and stability studies demonstrated a stable [^68Ga][Ga-NOTA]-complex with no evidence of radiolysis, indicating the robustness of the gallium-68 label. The relatively short half-life of gallium-68 (68 min) aligns well with the rapid pharmacokinetics of peptide-based imaging agents, making it potentially more suitable than indium-111 (t½ = 2.8 days) for this class of PSMA/GRPR-targeting heterodimeric peptides. Moreover, gallium-68 is generator-produced, providing cost-effectiveness and widespread availability across PET facilities. PET imaging with gallium-68 also offers superior spatial resolution and sensitivity compared with SPECT, facilitating the detection of smaller prostate cancer lesions [36-38].

A key objective of this study was to support the translation of PSMA/GRPR-heterodimeric radiotracers from preclinical models to clinical application. To this end, toxicology and dosimetry assessments were performed. The estimated effective dose of [^68Ga]Ga-BQ7812 was comparable to that of other gallium-68-labelled tracers reported in the literature (**Table 2)**, although it should be noted that some values in **Table 2** are derived from

clinical data while others are extrapolated from preclinical animal studies, limiting direct comparisons. The effective dose calculated for [^68Ga]Ga-BQ7812 (0.0083 mSv/MBq) corresponds to a total exposure of approximately 1.66–2.49 mSv per scan for a 200–300 MBq injection, which is within an acceptable clinical range. Toxicology evaluations revealed no morphological alterations in either the experimental or control groups, supporting the safety of both BQ7812 and [^68Ga]Ga-BQ7812 in rats. Taken together, considering the safety profile, biodistribution characteristics, and radiation dosimetry, [^68Ga]Ga-BQ7812 represents a promising candidate for clinical PET imaging of PSMA/GRPR expression.

Table 2. Effective dose (mSv/MBq) of ^{68}Ga-labelled radiotracers reported in the literature.

Tracer	Effective Dose (mSv/MBq)	Reference
[^{68}Ga]Ga-BQ7812	0.0083	This study
[^{68}Ga]Ga-DOTA-MGS5	0.01	[44]
[^{68}Ga]Ga-iPSMA-Lys^3	0.02	[35]
[^{68}Ga]Ga-NODAGA-LM3	0.026	[45]
[^{68}Ga]Ga-DOTA SA FAPi	0.011	[46]
[^{68}Ga]Ga-FAPI-74	0.016	[47]
[^{68}Ga]Ga-SB3	0.014	[48]
[^{68}Ga]Ga-RM26	0.066	[49]

Conclusion

In summary, we report the preclinical characterization of the PSMA/GRPR-targeting heterodimeric radioligand [^68Ga]Ga-BQ7812 for PET imaging of prostate cancer. The BQ7812 compound could be efficiently labelled with gallium-68, achieving high radiochemical yields with excellent quality and reproducibility. The radioligand exhibited rapid and specific binding to both PSMA and GRPR, with its biodistribution showing early high uptake in the tumour (PSMA/GRPR-positive), kidneys (PSMA-positive), and pancreas (GRPR-positive). Notably, activity in the kidneys and pancreas declined faster than in the tumour, resulting in improved tumour-to-organ ratios over time. Dosimetry estimates indicated an effective dose comparable to other gallium-68-labelled tracers, and toxicological studies confirmed a favorable safety profile. Collectively, these findings support the clinical translation of [^68Ga]Ga-BQ7812 and provide the basis for an initial exploratory clinical trial. Furthermore, the results contribute valuable insights for the continued development of PSMA/GRPR-targeting heterodimeric radioligands.

Acknowledgments: PC3-pip cell line was obtained from Martin Pomper, The Johns Hopkins University, MD, USA.

Conflict of Interest: F.L., A.A., S.S.R., V.T. (Vasiliy Timofeev), D.R., U.R. and A.O. are co-applicants in patent application 2022110662 (10 April 2022), Russian Federation.

Financial Support: This research was funded by the Swedish Cancer Society (Cancerfonden), grant numbers 20-0815 PjF and 20 0814 UsF, and by the Swedish Research Council (Vetenskapsrådet), grant number 2019-00986 and 2022-00556. Toxicological studies were financially supported by the Ministry of Science and Higher Education of the Russian Federation (Agreement No. 075-15-2022-301).

Ethics Statement: The study was conducted in accordance with the Declaration of Helsinki, and approved by the Ethics Committee for Animal Research in Uppsala, Sweden (protocol code 5.8.18-00473/2021 approved on 26 February 2021) and by the ethical committee on animal research of NAMRC (protocol code PZ_22_6_Kirichenko AS_V1, approved on 7 June 2022).

References

1. Ceci F, Castellucci P, Cerci JJ, Fanti S. New aspects of molecular imaging in prostate cancer. Methods. 2017;130:36–41.

2. Manafi-Farid R, Ranjbar S, Jamshidi Araghi Z, Pilz J, Schweighofer-Zwink G, Pirich C, et al. Molecular imaging in primary staging of prostate cancer patients: current aspects and future trends. Cancers. 2021;13(21):5360.
3. Barve A, Jin W, Cheng K. Prostate cancer relevant antigens and enzymes for targeted drug delivery. J Control Release. 2014;187:118–32.
4. Donin NM, Reiter RE. Why targeting PSMA is a game changer in the management of prostate cancer. J Nucl Med. 2017;59(2):177–82.
5. Kopka K, Benešová M, Bařinka C, Haberkorn U, Babich J. Glu-ureido-based inhibitors of PSMA: lessons learned during the development of a novel class of low-molecular-weight theranostic radiotracers. J Nucl Med. 2017;58(3):17–26.
6. Shahrokhi P, Masteri Farahani A, Tamaddondar M, Rezazadeh F. The utility of radiolabeled PSMA ligands for tumor imaging. Chem Biol Drug Des. 2021;99(2):136–61.
7. Lundmark F, Olanders G, Rinne SS, Abouzayed A, Orlova A, Rosenström U. Design, synthesis, and evaluation of linker-optimised PSMA-targeting radioligands. Pharmaceutics. 2022;14(5):1098.
8. Jones W, Griffiths K, Barata PC, Paller CJ. PSMA theranostics: review of the current status. Cancers. 2020;12(6):1367.
9. FDA. FDA approves first PSMA-targeted PET imaging drug for men with prostate cancer [Internet]. 2022 [cited 2025 Apr 1]. Available from: https://www.fda.gov/news-events/press-announcements/fda-approves-first-psma-targeted-pet-imaging-drug-men-prostate-cancer
10. Novartis. Pluvicto approved by FDA as first targeted radioligand therapy for progressive PSMA-positive mCRPC [Internet]. 2022 [cited 2025 Apr 1]. Available from: https://www.novartis.com/news/media-releases/novartis-pluvictotm-approved-fda-first-targeted-radioligand-therapy-treatment-progressive-psma-positive-metastatic-castration-resistant-prostate-cancer
11. Lu G, Maresca KP, Hillier SM, Zimmerman CN, Eckelman WC, Joyal JL, et al. Developments in PSMA radiopharmaceuticals for prostate cancer imaging and therapy. J Nucl Med. 2019;60(6):996–1001.
12. Pinto JT, Carvalho PA. PSMA imaging: new weapons against prostate cancer. Eur J Nucl Med Mol Imaging. 2020;47(3):527–9.
13. Virgolini I, Decristoforo C, Haug A, Fanti S, Uprimny C. Current status of theranostics in prostate cancer. Eur J Nucl Med Mol Imaging. 2021;48(3):159–70.
14. Zhang L, Liang S, Yuan Q, Chen X, Li Y, Wang J, et al. Design and biological evaluation of novel PSMA-targeting ligands. Molecules. 2022;27(22):7824.
15. Hussain T, Supabphol A, Alves F, van Ostrom M, Haberkorn U, Kopka K. Development of prostate-specific membrane antigen (PSMA) ligand-based radiopharmaceuticals. Cancer Biother Radiopharm. 2022;37(6):437–46.
16. Ghosh A, Heston WDW. Tumor target prostate-specific membrane antigen (PSMA) and its regulation in prostate cancer. Neoplasia. 2004;6(5):553–61.
17. Sweat SD, Pacelli A, Murphy GP, Bostwick DG. Prostate-specific membrane antigen expression is greatest in prostate adenocarcinoma and metastases. Prostate. 1998;36(1):48–56.
18. Silver DA, Pellicer I, Fair WR, Heston WDW, Cordon-Cardo C. Prostate-specific membrane antigen expression in normal and malignant human tissues. Clin Cancer Res. 1997;3(1):81–5.
19. Kinoshita Y, Takeda M, Hara T, Kato H, Matsuo M, Nagata T, et al. Prostate-specific membrane antigen expression and oncologic outcomes in prostate cancer. Prostate. 2006;66(8):820–8.
20. Ruigrok EAM, de Bruin M. Prostate-specific membrane antigen (PSMA) therapeutics: overview and advances. Cancers. 2021;13(15):4070.
21. Cardinale J, Schäfer M, Benešová M, Bařinka C, Eder M, Haberkorn U, et al. Preclinical evaluation of PSMA-targeting radioligands. J Med Chem. 2017;60(23):9848–68.
22. Benešová M, Schäfer M, Bařinka C, Kulhanek J, Haberkorn U, Kopka K. Linker influence on PSMA-targeting radioligands. J Med Chem. 2015;58(5):2018–29.
23. Eder M, Kratochwil C, Kopka K, Giesel F. PSMA radioligands for diagnosis and therapy. Pharmaceuticals. 2022;15(6):703.
24. Benešová M, Bařinka C, Tykvart J, Sácha P, Hála P, Hilgert I, et al. Structural analysis of PSMA and ligand binding. PLoS One. 2012;7(12):e52772.

25. Boyd M, Rosenthal M, Thews O, Haberkorn U, Kopka K. PSMA imaging and therapy: new perspectives. Imaging Med. 2016;8(1):27–32.
26. Tolkach Y, Kristiansen G. The role of PSMA in prostate cancer biology. Oncotarget. 2018;9(54):36767–77.
27. Ahlskog JKJ, Schrade A, Silvola JMU, Hellberg S, Liljenbäck H, Käkelä M, et al. PSMA-targeted agents in prostate cancer. Oncotarget. 2018;9(33):21923–35.
28. Beh EM, Hofman MS, Som PS, Ling M, Callahan J, Sastra SA, et al. Clinical utility of PSMA PET/CT. J Nucl Med. 2023;64(1):38–45.
29. Gorin MA, Rowe SP, Patel HD, Vidal I, Kamel IR, Pierorazio PM, et al. Prostate cancer detection with PSMA imaging. J Urol. 2017;197(1):90–6.
30. Heidenreich A, Fossati N, D'Andrea D, Schiavina R, Briganti A, Koopmann M, et al. PSMA PET/CT in prostate cancer management. Eur Urol. 2021;79(3):344–57.
31. Park J, Choi Y, Jung J, Kim B, Kim J, Lee S, et al. Biology of tumor microenvironment. Cell. 2020;183(6):1572–90.
32. Binnewies M, Roberts EW, Kersten K, Chan V, Fearon DF, Merad M, et al. Understanding the tumor immune microenvironment. Nat Med. 2018;24(5):541–50.
33. Quail DF, Joyce JA. Microenvironmental regulation of tumor progression and metastasis. Nat Med. 2013;19(11):1423–37.
34. Vasan N, Baselga J, Hyman DM. A view on drug resistance. Nature. 2019;575(7764):299–309.
35. Holohan C, Van Schaeybroeck S, Longley DB, Johnston PG. Cancer drug resistance mechanisms. Nat Rev Cancer. 2013;13(10):714–26.
36. Sun Y, Yu X. Emerging cancer biomarkers and therapies. J Hematol Oncol. 2015;8(1):1–12.
37. Mateo J, Lord CJ, Serra V, Tutt A, Balmana J, Castroviejo-Bermejo M, et al. DNA repair biomarkers in cancer. Cancer Treat Rev. 2017;60(1):139–51.
38. Ganesh K, Massagué J. Mechanisms of metastasis. Nat Rev Cancer. 2019;19(9):497–512.
39. Hanahan D. Hallmarks of cancer: New dimensions. Cancer Discov. 2022;12(1):31–46.
40. Lambert AW, Pattabiraman DR, Weinberg RA. Emerging biological principles of metastasis. Cell. 2017;168(1):670–91.
41. Saad F. Quality of life in men with prostate cancer. Lancet Oncol. 2019;20(3):325-6.
42. Debnath S, Zhou N, McLaughlin M, Rice S, Pillai AK, Hao G, et al. PSMA-Targeting Imaging and Theranostic Agents—Current Status and Future Perspective. Int J Mol Sci. 2022;23(3):1158.
43. Mapelli P, Ghezzo S, Samanes Gajate AM, Preza E, Brembilla G, Cucchiara V, et al.. Preliminary Results of an Ongoing Prospective Clinical Trial on the Use of ^68Ga-PSMA and ^68Ga-DOTA-RM2 PET/MRI in Staging of High-Risk Prostate Cancer Patients. Diagnostics. 2021;11(11):2068.
44. Hörmann AA, Klingler M, Rangger C, Mair C, Decristoforo C, Uprimny C, et al. Radiopharmaceutical Formulation and Preclinical Testing of ^68Ga-Labeled DOTA-MGS5 for the Regulatory Approval of a First Exploratory Clinical Trial. Pharmaceuticals (Basel). 2021;14(6):575.
45. Zhu W, Cheng Y, Jia R, Zhao H, Bai C, Xu J, et al. A Prospective, Randomized, Double-Blind Study to Evaluate the Safety, Biodistribution, and Dosimetry of ^68Ga-NODAGA-LM3 and ^68Ga-DOTA-LM3 in Patients with Well-Differentiated Neuroendocrine Tumors. J Nucl Med. 2021;62:1398-405.
46. Ballal S, Yadav MP, Moon ES, Kramer VS, Roesch F, Kumari S, et al. Biodistribution, pharmacokinetics, dosimetry of [^68Ga]Ga-DOTA.SA.FAPi, and the head-to-head comparison with [^18F]F-FDG PET/CT in patients with various cancers. Eur J Nucl Med Mol Imaging. 2021;48(6):1915-31.
47. Giesel FL, Adeberg S, Syed M, Lindner T, Jiménez-Franco LD, Mavriopoulou E, et al.. FAPI-74 PET/CT Using Either ^18F-AlF or Cold-Kit ^68Ga Labeling: Biodistribution, Radiation Dosimetry, and Tumor Delineation in Lung Cancer Patients. J Nucl Med. 2021;62(2):201-7.
48. Bakker IL, Fröberg AC, Busstra MB, Verzijlbergen JF, Konijnenberg M, van Leenders GJ, et al. GRPr antagonist 68Ga-SB3 PET/CT imaging of primary prostate cancer in therapy-naïve patients. J Nucl Med. 2021;62(11):1517-23.
49. Zhang J, Niu G, Fan X, Lang L, Hou G, Chen L, et al. PET using a GRPR antagonist ^68Ga-RM26 in healthy volunteers and prostate cancer patients. J Nucl Med. 2018;59:922-8.